Regulation of PPARα by APP in Alzheimer disease impacts the pharmacological modulation of synaptic activity

Francisco Sáez-Orellana, Thomas Leroy, Floriane Ribeiro, Anna Kreis, Karelle Leroy, Fanny Lalloyer, Eric Baugé, Bart Staels, Charles Duyckaerts, Jean-Pierre Brion, et al.

JCI insight

Regulation of PPARα by APP in Alzheimer disease impacts the pharmacological modulation of synaptic activity

Francisco Sáez-Orellana, … , Jean-Noël Octave, Nathalie Pierrot

JCI Insight. 2021. https://doi.org/10.1172/jci.insight.150099.

Research In-Press Preview Neuroscience

Graphical abstract

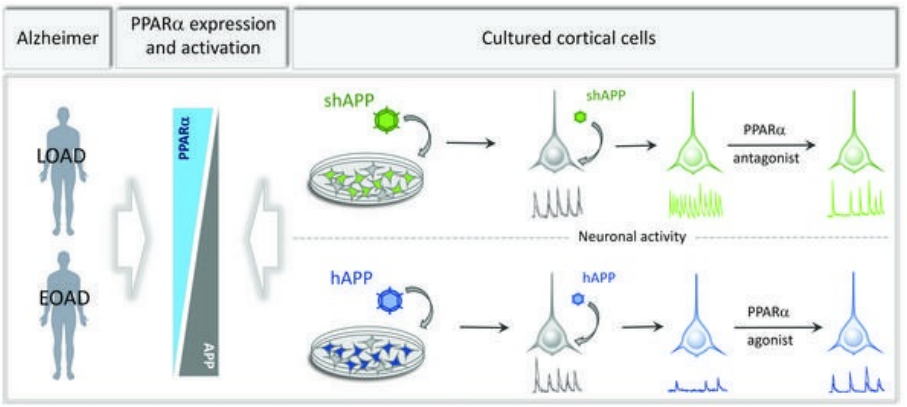

Title:

Regulation of PPARα by APP in Alzheimer disease impacts the pharmacological modulation of synaptic activity.

Authors and affiliations:

Francisco Sáez-Orellana[1†], Thomas Leroy[1], Floriane Ribeiro[1], Anna Kreis[2], Karelle Leroy[3], Fanny Lalloyer[4], Eric Baugé[4], Bart Staels[4], Charles Duyckaerts[5], Jean-Pierre Brion[3], Philippe Gailly[2], Jean-Noël Octave[1] and Nathalie Pierrot[1,†,*].

[1] Université catholique de Louvain, Institute of Neuroscience, Alzheimer Dementia group, B-1200 Brussels, Belgium.

[2] Université catholique de Louvain, Institute of Neuroscience, Laboratory of Cell Physiology, B-1200 Brussels, Belgium.

[3] Université libre de Bruxelles, Laboratory of Histology and Neuropathology, 1070 Brussels, Belgium.

[4] Univ. Lille, Inserm, CHU Lille, Institut Pasteur de Lille, U1011, F-59000 Lille, France.

[5] Sorbonne Université, Hôpital de la Pitié-Salpêtrière, Paris Brain Institute (ICM), CNRS UMR7225, INSERM U1127, 75013 Paris, France.

† These authors contributed equally to this work.

* Correspondence: Nathalie Pierrot, Université catholique de Louvain, Institute of Neuroscience, Alzheimer Dementia, avenue Mounier 53, SSS/IONS/CEMO-Bte B1.53.03, B-1200, Brussels, Belgium. Office: +32 2 764 93 34, E-mail: nathalie.pierrot@uclouvain.be

Thomas Leroy's present affiliation: VIB Center for Brain and Disease Research & KU Leuven, Department of Neurosciences, Gasthuisberg, B-3000 Leuven, Belgium

Conflict of interest statement:

The authors have declared that no conflict of interest exists.

Abstract

Among genetic susceptibility loci associated with late-onset Alzheimer disease (LOAD), genetic polymorphisms identified in genes encoding lipid carriers led to the hypothesis that a disruption of lipid metabolism could promote disease progression. We previously reported that amyloid precursor protein (APP) involved in AD physiopathology impairs lipid synthesis needed for cortical networks activity and that activation of peroxisome proliferator-activated receptor α (PPARα), a metabolic regulator involved in lipid metabolism, improves synaptic plasticity in an AD mouse model. These observations led us to investigate a possible correlation between PPARα function and full-length APP expression. Here, we report that PPARα expression and activation are inversely related to APP expression both in LOAD brains and in early-onset AD cases with a duplication of the *APP* gene, but not in control human brains. Moreover, human APP expression decreased *PPARA* expression and its related target genes in transgenic mice and in cultured cortical cells, while opposite results were observed in APP silenced cortical networks. In cultured neurons, APP-mediated decrease or increase in synaptic activity was corrected by PPARα specific agonist and antagonist, respectively. APP-mediated control of synaptic activity was abolished following PPARα deficiency, indicating a key function of PPARα in this process.

Introduction

Alzheimer's disease (AD) is the most common form of dementia, accounting for nearly 70% of the cases worldwide (1). AD is characterized by the presence in the brain of neurofibrillary tangles containing paired helical filaments of hyper-phosphorylated tau protein and senile plaques, with an amyloid core of amyloid β (Aβ) peptide derived from the amyloid precursor protein (APP) (2). Synaptic dysfunction seems to occur long before the presence of these neuropathological lesions in the brain of AD patients and might contribute to cognitive dysfunction (3). Autosomal dominant mutations found in *APP* gene or genes encoding presenilins, involved in the γ-secretase-mediated processing of APP into Aβ, account for the majority of rare inherited early-onset AD cases (EOAD), in which Aβ is considered as the main culprit of the pathology (1). However, genome-wide association studies have identified dozens of genetic susceptibility loci that are associated with higher risk for late-onset AD (LOAD) (4). Among the most important AD genetic risk factors, genetic polymorphisms found first in *APOE* and later in *CLU* and *ABCA7* genes encoding lipid carriers (4), led to the hypothesis that a disruption of lipid metabolism could promote disease progression (5). This hypothesis is sustained by findings reporting that genetic polymorphisms in *SREBF* and *PPARA* genes, involved in cholesterol and fatty acid (FA) metabolism, were associated with an increased risk of LOAD (6-8), although the association between the genetic polymorphism identified in *PPARA* encoding the Peroxisome Proliferator-Activated Receptor α (PPARα) and AD is controversial (9). However, several LOAD genetic risk factors are involved in pathways that are governed by PPARα, highlighting a potential link between PPARα and the etiology of AD (reviewed in (10)). PPARα belongs to the nuclear receptor superfamily of ligand-dependent transcription factors and is broadly implicated in a wide variety of biological processes regulating energy balance, inflammation, FA and glucose metabolism (11), a set of pathways

previously reported to be also disturbed in LOAD (12-14). More recently, a potential role of PPARα in cognition emerged. Spatial learning and long-term memory deficits observed in PPARα-knockout mice indicate that PPARα is required for normal cognitive function (15). Moreover, PPARα deficiency affects the expression of a set of synaptic-related proteins involved in excitatory neurotransmission (16) and severely impairs hippocampal long-term potentiation (LTP) (17), an activity-dependent enhancement of synaptic strength involved in memory processing (18). Accordingly, a growing body of evidence reports that activation of PPARs has salutary effects on neurodegenerative disorders including AD (19). Administration of PPARα activators reduces AD-like pathology and cognitive decline in murine models of AD overexpressing mutated human APP and presenilin 1 linked to familial AD (17, 20, 21). Inasmuch as PPARs expression is modified in AD brains (22), we hypothesized that the function of PPARα could be impaired in AD and may therefore contribute to the progression of the disease.

In this study, we report that *PPARA* mRNA level and the expression of PPARα related target genes are modified in brains from LOAD and EOAD cases with a rare *APP* duplication and that *PPARA* expression inversely correlated with the expression of human APP (hAPP) protein in AD. We previously demonstrated that increased expression of hAPP in cortical cells inhibits both cholesterol turnover and FA biosynthesis needed for neuronal network activity (23). In addition, we observed that PPARα deficiency leads to decreased LTP as well (17). Therefore, we have investigated whether modification in *PPARA* expression could be mediated by APP expression levels. We report that *PPARA* mRNA and expression of related PPARα downstream target genes are decreased in transgenic mice and in cultured cortical cells overexpressing non-mutated human APP, while opposite results were observed in APP silenced cortical networks. Moreover, APP-mediated effects on *PPARA* expression and thereby on synaptic activity were reversed with PPARα specific modulators in cultured cortical cells.

Results

Human APP-dependent expression and i of PPARα in brains from patients with late-onset Alzheimer disease and in early-onset cases with a duplication of the *APP* locus.

We first analysed the expression of *PPARA* mRNA level in human post-mortem brains from controls and late-onset AD cases (LOAD) (**Supplemental Table 1**). A 3-fold increase in the relative expression of *PPARA* (2.88 ± 0.63) was observed in the frontal cortex of LOAD compared to non-demented control samples (**Figure 1A**). We next analysed the activation of PPARα in control and LOAD samples by measuring mRNA level of *ACOX1*, the first identified target gene of PPARα that encodes Acyl-CoA Oxidase 1, a rate-limiting enzymes involved in peroxisomal FA oxidation (11). A 5-fold increase in the relative expression of *ACOX1* (4.95 ± 1.07) gene was measured in the frontal cortex of LOAD samples compared to controls (**Figure 1B**). The huge variability in the increased expressions of *PPARA* and *ACOX1* measured in AD brains prompted us to analyse a possible correlation between *PPARA* and *ACOX1* mRNA expressions in LOAD. We observed a strong correlation between PPARα expression (*PPARA* mRNA) and activation (*ACOX1* expression) in LOAD (**Figure 1C**). Moreover, we observed that the *CPT1A* (4.97 ± 1.37) gene encoding Carnitine Palmitoyltransferase 1A, a rate-limiting enzymes involved in mitochondrial FA oxidation (11), and *PDK4* (3.83 ± 0.81) encoding Pyruvate Dehydrogenase Kinase 4, which regulates the rate-limiting step of glucose oxidation by switching off the pyruvate dehydrogenase complex (24), were also increased in the frontal cortex of LOAD compared to non-demented control samples (**Supplemental Figure 1A**), two non-specific PPARα genes known to be nevertheless regulated by PPARα (11). Inasmuch as *ACOX1, CPT1A* and *PDK4* expressions are related to FA and glucose oxidation, these results corroborate abnormalities in brain FA and glucose metabolism, bioenergetics, and mitochondrial function reported in AD (12, 13, 25). Since lipid biochemistry is disrupted in AD

(10, 26) and given that one of the main neuropathological characteristics involved in AD pathogenesis implies the APP protein (27, 28), which we have previously reported to decrease both cholesterol and FA biosynthesis when its expression level increases (23), we wondered whether modifications in *PPARA* expression observed could be related to human APP (hAPP) expression. While the global expression level of full-length hAPP protein was unchanged in LOAD compared to controls (**Figures 1D** and **1E**), a case by case analysis reveals a tight inverse correlation between hAPP protein and *PPARA* expressions in LOAD, but not in control brains (**Figures 1F** and **1G**), suggesting that *PPARA* expression is regulated by hAPP expression level only in LOAD. From these results, we next analysed *PPARA* and PPARα downstream target genes expressions in human brains samples from rare early-onset AD (EOAD) cases with a microduplication in the *APP* locus (**Supplemental Table 2**) (27, 29). *PPARA*, *ACOX1*, *CPT1A* and *PDK4* mRNA levels were 3 to 4-fold decreased (0.35 ± 0.15, 0.22 ± 0.09, 0.37 ± 0.10, 0.22 ± 0.15, respectively) (**Figures 1H**, **1I** and **Supplemental Figure 1B**) in EOAD cases compared to controls, in whom a two-fold increase in brain hAPP protein expression (2.13 ± 0.25) was observed compared to age-matched controls (**Figures 1J** and **1K**), supporting therefore that increase in hAPP expression was concomitant with decrease in *PPARA*. Altogether these results suggest that non-mutated hAPP expression is inversely correlated with the expression of *PPARA* and PPARα target genes both in LOAD and EOAD cases, but not in control human brains.

Brain *Ppara* expression and its downstream target genes are decreased in transgenic mice overexpressing wildtype human APP.

Among transgenic mouse models created to gain insight into AD pathology, the most commonly used are those overexpressing mutated hAPP linked to familial AD (30) resulting in the formation of brain amyloid plaques, one of the pathological hallmarks observed in the brain

of AD patients. Because of their intrinsic relationship, the impact of hAPP expression on *Ppara* expression was separated from that of amyloid deposition by studying the hemizygous transgenic mouse model overexpressing wildtype form of hAPP ($hAPP_{WT}$ formerly known as line I5 mouse strain (31)), a mouse model displaying spatial learning and memory deficits with high cortical level of hAPP and no evidence for Aβ deposition (31, 32). By western blot analysis with an antibody that recognizes human and mouse APP, 2 to 3-fold higher APP levels were observed in $hAPP_{WT}$ as compared to WT mice at early (3-4 months old: 2.67 ± 0.34), advanced (6-8 months old: 1.86 ± 0.21) and late ages (11-12 months old: 2.63 ± 0.30) (**Figure 2A** and **2B**) as expected (32). A trend of a higher expression of brain *Ppara* was observed together with a trend of increased *Acox1, Cpt1a* and *Pdk4* mRNA levels along with age in WT mice (**Figures 2C - 2F**), indicating that the aged brain retains enhanced FA utilization compared to young WT mice, meaning that aging brain could switch to FA oxidation (33, 34). While a similar profile was observed in $hAPP_{WT}$ mice at early and advanced ages, a 2 to 5-fold decrease in *Ppara*, *Acox1*, *Cpt1a* and *Pdk4* mRNA levels was observed (0.46 ± 0.04, 0.58 ± 0.06, 0.50 ± 0.10, 0.91 ± 0.06, respectively) in 11-12 months old $hAPP_{WT}$ mice compared to WT littermates at the same age (**Figures 2C - 2F**), an age at which severe cognitive deficits are detected (32, 35). Metabolic alterations including deficits for acylcarnitines have previously been reported in brain of a transgenic mouse model of AD bearing mutated APP and PS1 transgenes, in which early brain amyloid deposition and cognitive impairment occur (36). Nevertheless, our results indicate that in absence of amyloid deposition, non-mutated hAPP overexpression is sufficient to induce a decrease in brain *Ppara* expression and its downstream target genes and suggest therefore that activation of β-oxidation pathways of FA in the mitochondria might be perturbed in the brain of APP_{WT} mice. Moreover, besides hAPP overexpression, an additional age-dependent contribution is needed to observe a decrease in the expression of PPARα downstream target

genes, a decrease similar to that previously observed in human brain samples with *APP* duplication.

Wy14643 PPARα agonist prevents human APP-induced decreases in PPARα activation and synaptic activity in cortical cultures.

The finding that activation of all PPARs, but especially PPARγ, has salutary effects on neurodegenerative disorders including AD (19) and that a promising role of PPARα in AD therapy emerged (10, 37), we wondered whether PPARα specific agonist could interfere with hAPP-mediated decrease in PPARα target genes expression observed. To address this question, we expressed neuronal wild-type hAPP isoform in cultured rat cortical cells. Full-length hAPP expression was achieved by transducing primary cortical cultures with a recombinant adenoviral vector at 6 DIV and hAPP expression was probed by immunoblotting at 13-14 DIV with the hAPP specific WO2 antibody (**Figure 3A**). We have previously shown that transgene expression was homogeneous, did not affect cell density and viability and remained stable over time (38). By using an antibody that recognizes both human and endogenous rat APP, a nearly 2-fold increase in total APP levels (1.87 ± 0.15) was observed compared to control cells transduced with an adenovirus encoding the human recombinant green fluorescent protein (hrGFP) (**Figure 3A** and **3B**). As previously observed in human and mouse brain lysates overexpressing hAPP protein, *Ppara* (0.49 ± 0.05), *Acox1* (0.40 ± 0.06), *Cpt1a* (0.39 ± 0.06) and *Pdk4* (0.46 ± 0.10) mRNA levels were reduced by about 60 % in hAPP expressing cells compared to hrGFP vehicle treated controls (**Figure 3C** and **3D**). It is very well known that cancers reprogram their metabolism to adapt to environmental changes. Cpt1a fuels lipid beta-oxidation by producing acyl-carnitines in the mitochondria (39). It was recently demonstrated that in prostate cancer cell models, overexpression of *Cpt1a* is associated with a significant increase in intracellular lipase activity (40), a step which liberates fatty acids from triglyceride

stores which can then be used for β-oxidation (41). Consequently, overexpression of *Cpt1a* increases free fatty acid (FFA) content in these cancer cells. We measured whether modification in Cpt1a expression influences FFA content in our cultured cortical cells. In hAPP expressing cells, a decrease in *Cpt1a* expression was concomitant with a 70 % decrease in cell FFA content (0.32 ± 0.06) compared to hrGFP control (**Supplemental Figure 2A**), demonstrating that modification in *Cpt1a* expression affects fatty acids metabolism in our cortical cells in culture. Moreover, since Pdk4 is known to play a role in the metabolic switch from glycolysis to mitochondrial oxidative phosphorylation (OXPHOS) (24), decrease in *Pdk4* observed indicates that hAPP expression enhances glycolysis in cortical cells (42). Cells were then treated with pirinixic acid (Wy14643), a synthetic PPARα agonist (reviewed in (19, 43)). As expected, the basal expression of *Acox1* (1.66 ± 0.16), *Cpt1a* (1.72 ± 0.21), and *Pdk4* (1.61 ± 0.16) genes were increased in Wy14643 treated hrGFP cells compared to vehicle treated cells (**Figure 3D**). Moreover, Wy14643 was able to inhibit the hAPP-mediated decrease in *Acox1*, *Cpt1a*, and *Pdk4* mRNA levels (**Figure 3D**), indicating that the pharmacological modulation of PPARα is able to restore hAPP-mediated effects on PPARα target genes expression in cortical cells in culture.

As PPARα deficiency affects neuronal activity in cultured hippocampal neurons (16) and synaptic plasticity in mice (17), we hypothesized that decrease in PPARα target genes expression could contribute to the hAPP-mediated synaptic transmission silencing of cortical networks (23, 44, 45). To study the effect of 5-7 days hAPP expression on synaptic activity, we performed whole-cell voltage clamp recordings. Resting membrane potential (RMP) was more negative (ΔVm −8.04 mV ± −1.16) (38) (**Figure 3E**) and concomitant decreases in spontaneous total synaptic activity (**Figure 3F**) frequency (hrGFP, 1.50 ± 0.37 Hz; hAPP, 0.21 ± 0.06 Hz; **Figure 3G**) and amplitude averages (hrGFP, 32.41 ± 1.30 pA; hAPP, 20.93 ± 1.22 pA, **Figure 3H**) were measured in hAPP neurons compared to hrGFP controls. However, Wy14643

treatment partially prevented the effect of hAPP expression on synaptic activity (**Figure 3F**), restored RMP and increased both frequency (vehicle hAPP, 0.21 ± 0.06 Hz; Wy14643 hAPP, 2.58 ± 0.51 Hz) and amplitude of synaptic events (vehicle hAPP, 20.93 ± 1.22 pA; Wy14643 hAPP, 27.79 ± 0.67 pA), while no significant changes were observed in Wy14643 hrGFP compared to vehicle treated controls (**Figures 3E, G and H**). Altogether, these results indicate that PPARα activation with a specific agonist can prevent hAPP-mediated synaptic activity depression of cortical networks.

GW6471 PPARα antagonist inhibits APP knockdown-induced increases in PPAR activation and synaptic activity in cortical cultures.

To further investigate the possible modulation of PPARα activation by APP, APP expression was reduced in cortical cells by using shRNA construct designed to target endogenous APP (shAPP). The knockdown of endogenous rat APP was achieved by transducing cells on 6 DIV with recombinant lentiviruses encoding shAPP and a scrambled shRNA encoding GFP (shScra-GFP) was used as a negative control. At 13-14 DIV, blots were probed with an antibody that recognizes the 19 carboxyl-terminal amino acids of endogenous APP (**Figure 4A**). As expected, a 66.66 ± 5.7 % reduction of endogenous APP expression (38) (**Figure 4B**) with no induction in the expression of APLP1 and APLP2 for functional compensation for the loss of APP were observed as we have previously reported (23, 38). Unlike hAPP cells, APP knockdown induced a 2-fold increase in *Ppara* (1.89 ± 0.26), *Acox1* (2.19 ± 0.24) and *Cpt1a* (1.98 ± 0.18) and robustly increased *Pdk4* (4.22 ± 0.63) mRNA levels compared to controls (**Figure 4C** and **4D**), indicating that PPARα activation is increased in these cells. Contrary to hAPP expressing cells, an increase in *Cpt1a* expression was concomitant with a 75% increase in FFA content (1.75 ± 0.10) in shAPP cells compared to shScra-GFP control cells (**Supplemental Figure 2B**). These results confirm that APP-mediated modification in *Cpt1a* expression affects fatty acids

metabolism in cortical cells. Moreover, these results suggest that reduction in endogenous APP enhances the transport of FAs into the mitochondria for β-oxidation and that shAPP cells may be less glycolytic (46). We next used GW6471 to specifically inhibit PPARα activity (47) in order to counteract the shAPP-mediated effect on PPARα activation. The effectiveness of GW6471 was confirmed by the decreased expression of *Cpt1a* observed in both treated shAPP (0.69 ± 0.18) and shScra-GFP (0.41 ± 0.06) cells compared to vehicle-treated controls (**Figure 4C**), while no changes were observed in *Acox1* and *Pdk4* mRNA levels. These results indicate that the GW6471 PPARα antagonist partially inhibits APP knockdown-induced increase in PPARα activation and specifically affects *Cpt1a* expression in cortical cells.

To address whether increase in PPARα activation could contribute to shAPP-mediated increase in neuronal activity of cortical networks as reported (23), we performed whole-cell voltage clamp recordings in APP knocked down neurons and treated them with GW6471. RMP was more positive (ΔVm $-11.20\,\text{mV} \pm -0.22$) (**Figure 4E**) and concomitant increase in total synaptic activity (**Figure 4F**) frequency (shScra-GFP, 1.30 ± 0.06 Hz; shAPP, 2.55 ± 0.27 Hz; **Figure 4G**), with no significant change in the amplitude (shScra-GFP, 51.89 ± 10.49 pA; shAPP, 51.42 ± 3.09 pA, **Figure 4H**), was measured in shAPP compared to shScra-GFP controls. Moreover, GW6471 restored RMP, frequency and amplitude in treated shAPP to levels similar to vehicle treated controls (**Figures 4E-H**). Altogether, these results indicate that APP expression levels modulate the activation of PPARα and thereby synaptic function and that pharmacological approaches targeting PPARα allow to reverse APP mediated effects observed in cortical cells in culture.

Control of synaptic activity by APP disappears in the absence of PPARα in cortical cultures.

To address whether APP-mediated control of synaptic activity could be PPARα dependent, primary cultures of cortical cells derived from WT and PPARα deficient (*Ppara*$^{-/-}$) mice (**Figure 5A**) were transduced with recombinant viruses in order to express hAPP (**Figure 5B**) or to repress endogenous APP (**Figure 5C**). With a similar extent as observed previously in rat primary cultures, a two fold increase (2.22 ± 0.25) and a 60 % reduction (0.40 ± 0.02) in total APP levels were observed in hAPP and shAPP WT relative to infected WT controls. Moreover, PPARα deficiency did not affect total APP content increase (2.24 ± 0.22) and decrease (0.45 ± 0.05) observed in hAPP and shAPP *Ppara*$^{-/-}$ compared to hAPP and shAPP WT, respectively (**Figure 5D**). Although the knockout of PPARα increased averages of total synaptic activity frequency (4.34 ± 0.51 Hz) and amplitude (64.47 ± 3.45 pA) in all infected conditions, PPARα deficiency totally prevented APP-mediated effects on RMPs, synaptic events frequencies and amplitudes recorded in hAPP and shAPP *Ppara*$^{-/-}$ compared respectively to hrGFP and shScra-GFP controls (**Figures 5E-H**). Altogether, these results suggest that PPARα is a downstream mediator of APP-mediated control on synaptic activity.

Discussion

We report here that *PPARA* expression and PPARα downstream target genes are inversely correlated with hAPP expression in both LOAD and EOAD with a microduplication of the *APP* locus. Such an effect of hAPP expression was also observed in hAPP transgenic mice and in cortical networks, in which pharmacological approaches targeting PPARα alleviate APP-mediated synaptic dysfunction.

The overall increase in the expression of *PPARA mRNA* that we have observed in LOAD is not in agreement with previous results reporting globally reduced expression level of PPARα in AD brains (22). However, a case by case analysis reveals a tight inverse correlation between hAPP protein and *PPARA* expressions in our LOAD samples, but not in control brains, suggesting that *PPARA* expression is regulated by hAPP expression level only in LOAD. The large variability of both hAPP protein and *PPARA* mRNA contents observed in the LOAD group could probably account in part for the discrepancy with the results published by de la Monte and colleagues (22). Expression, trafficking and processing of APP are regulated in a complex way including prominent changes during pathological states. It was previously reported that APP expression is upregulated under conditions of metabolic stress (48), ischemia (49), brain injury (50) and inflammation (51) and that individual APP expression is heterogeneous in AD patients (49). Moreover, our results put forward that APP expression seems to play a determining role on *PPARA* expression in LOAD, but not in controls, in which no correlation between hAPP and *PPARA* mRNA contents was observed. Furthermore, our results demonstrate that in addition to *PPARA* gene expression, expression of *ACOX1*, *CPT1A* and *PDK4* PPARα target genes, are inversely correlated with hAPP expression when LAOD samples are analysed individually. This inverse correlation between hAPP and *PPARA* expression and activation is confirmed in EOAD cases with a rare duplication of the *APP* locus.

We conclude that particular attention should be paid to the level of hAPP expression in each AD case studied when the expression of *PPARA* is considered. Such an inverse correlation between hAPP and *PPARA* expression was not observed in control brains, indicating a specific function of hAPP in AD.

In the brain of AD patients, microglial activation is observed in the vicinity of senile plaques at all stages of the disease and is accompanied by increased levels of pro-inflammatory molecules (*e.g.* TNF, IL-1β, IL-6, prostaglandins) (52). Genome-wide association studies identified inflammation-related genes as potential risk factors for developing AD (53). In addition, it was recently reported that APP expression is increased under inflammatory processes in an AD transgenic mouse model (51). Therefore, we cannot exclude that inflammation could mediate changes in brain APP expression that could thereby affect *PPARA* expression in AD samples analysed.

Increases in *ACOX1* and *CPT1A* observed in LOAD with a low hAPP content indicate that β-oxidation pathways of very long chain FA in the peroxisome and short-, medium-, and long-chain fatty acids in the mitochondria are activated. Activation of FA oxidation might take place to compensate for compromised pyruvate dehydrogenase complex (PDC) to provide alternative sources of acetyl-CoA to sustain ATP energy supply. Indeed, a concomitant increase in the expression of *PDK4* that catalyses the phosphorylation-dependent inactivation of the mitochondrial PDC (24) was observed in LOAD, in whom a reduction in PDC activity was previously reported (54). As mitochondrial PDC connects glycolysis to oxidative metabolism (55) and as PDK4 up-regulation facilitates FA oxidation, in particular when glucose is scarce during energy deprivation (56), *PDK4* increase observed in LOAD brain correlates with the reduced cerebral glucose utilization found in AD patients (12), in which early brain peroxisomal and mitochondrial function deficits have been reported (reviewed in (22, 57)). Although a shift

in brain metabolism from glucose-driven energy supply to a ketogenic/FA oxidation pathways is reported in LOAD (58), this shift could depend on the level of APP expression. In addition, an opposite shift may take place in EOAD carrying a microduplication of the *APP* locus (27, 29). Indeed, an inverse correlation was observed in brain samples from *APP*dup cases, in which increase in hAPP is concomitant with decreases in *PAPARA*, *ACOX1*, *CPT1A* and *PDK4* expression. We conclude that metabolic shifts observed in LOAD and EOAD could rely on hAPP expression level, suggesting that hAPP by controlling *PPARA* expression and its downstream target genes might be considered as an essential metabolic mediator in AD, but not in control brains. Although modifications in brain *PAPARA*, *ACOX1*, *CPT1A* and *PDK4* expression observed could be mediated by variations in hAPP expression in AD, a role for hAPP cleavage products including Aβ, tau phosphorylation, brain inflammation, synaptic loss and amyloid burden reported in AD brains cannot be ruled out (2).

Interestingly, neuropathological changes observed in AD were reported in patients with Down syndrome (DS), in whom the presence of an extra chromosome 21 leads to intellectual disability. Association between AD and DS is partially due to the overexpression of hAPP that results from the location of *APP* gene on chromosome 21 (59). Moreover, mitochondrial deficits, increase in oxidative stress, impaired glucose and lipid metabolism leading to a reduced rate of energy metabolism were reported in DS (reviewed in (60)). Recently, severe brain malformations with pyruvate dehydrogenase deficiency and DS were reported (61) and the Down syndrome critical region 2 protein was shown to inhibit the transcriptional activity of PPARβ in cell line, indicating a potential dysfunction of PPAR activation in DS, in which hAPP expression level is increased (62).

APP-dependent modulation of brain *PPARA, ACOX1*, *CPT1A* and *PDK4* expression was not only observed in human AD brain but also in mice. Indeed, we show that overall increase in

APP expression lowers brain *Ppara* expression and thereby *Acox1*, *Cpt1* and *Pdk4* in $hAPP_{WT}$ mice at late stages (31, 32). An increase in Acox1 expression was found in the hippocampus of young Tg2576 mice, a mouse model of AD harbouring the human Swedish familial AD mutation that develops parenchymal amyloid plaques at 11-13 months of age, while Acox1 expression was found to be decreased in old animals (63, 64). Moreover, *Pdk4* decrease observed in old $hAPP_{WT}$ mice corroborates the decrease in the PDC reported in brain synaptosomes of Tg2576 mice (65). However, decreases in *Acox1* and *Pdk4* observed in APP_{WT} mice rule out a possible involvement of amyloid plaques in these mice, which are devoid of brain Aβ deposition (31, 32).

APP-dependent regulation of *Ppara, Acox1*, *Cpt1a* and *Pdk4* mRNA observed in $hAPP_{WT}$ mice, EOAD with a duplication of the *APP* locus and LOAD cases were recapitulated in hAPP expressing and silenced APP cultured cortical cells, indicating a critical involvement of APP expression in the regulation of *Ppara* and its downstream target genes. The diminution of *Pdk4* observed in hAPP expressing cells indicates that hAPP expression and/or increase in total APP content enhances glycolytic metabolism, as reported in human neuroblastoma cells in which increase in neuronal hAPP levels mediates an Aβ-independent Pdk4 downregulation (42). Conversely, the robust *Pdk4* increase observed in APP-silenced cortical cells suggests that APP reduction lowers cell glycolytic capacity (46). Variations in APP expression therefore modulate *Ppara* expression and its downstream target genes in cultured cortical cells, strengthening a potential role of APP expression as metabolic mediator. Moreover, a pivotal role of Pdks and metabolic flexibility was reported in the brain that utilizes glucose as primary energy source (24). Astrocytes expressed more Pdks than neurons and have lower PDC activity (66), indicating that APP-mediated changes in Pdk4 expression might occur primarily in astrocytes in our cultured cells. Moreover, increase in *Cpt1a* observed in APP knocked down cells takes

place also probably in astrocytes (33), in which FA oxidation predominantly occurs to contribute up to 20% of the total brain energy requirement as reported in brain primary cultures (67). Given that there is a tight metabolic coupling between astrocytes and neurons, a metabolic transition from glycolysis to OXPHOS could occur in APP knocked down cells to provide adequate ATP level to meet the increased energy demand needed for the sustained synaptic activity observed.

While we observed a depressive effect of hAPP expression on synaptic transmission that could result from an Aβ-dependent postsynaptic silencing of α-amino-3-hydroxy-5-methyl-4-isoxazolepropionic acid (AMPA) (45) and N-methyl-D-aspartate (NMDA) receptor-mediated currents (44), synaptic excitatory transmission increased in APP-silenced neurons suggests that changes in neuronal activity drive changes in metabolic flux or vice versa. While energy metabolism of neurons is mainly aerobic and that of astrocytes mainly anaerobic glycolysis, OXPHOS was shown to be the main mechanism initially providing energy to power neuronal activity (68). Accordingly, miniature excitatory postsynaptic currents frequency was shown to be increased in neurons derived from APP knock-out mice (69), in which a resistance to a high fat diet (HFD)-induced obesity was observed and linked to higher energy expenditure and lipid oxidation (70). Moreover, changes in synaptic activity observed could be mediated by the Cpt1c isoform. Indeed, despite the inability of the brain specific Cpt1c isoform to β-oxidize long chain FAs contrary to Cpt1a (71), Cpt1c could enhance whole-cell currents of shAPP neurons by increasing the trafficking and the surface expression of the GluA1 subunit containing AMPA receptors to enhance AMPA receptors mediated currents (71).

Our findings also put forward that APP-mediated changes in the expression of *Acox1*, *Cpt1a* and *Pdk4* are driven by metabolic regulators and in particular PPARα. The central role of PPARα in FA catabolism is very well known (11). PPARα increases expression of genes

encoding peroxysomal and mitochondrial enzymes including Acox1 and Cpt1 and both PPARα and PPAR-β/δ but not PPAR-γ also activate the Pdk4 encoding gene (11). We report that PPARα modulators are able to reverse APP mediated effects observed in cultured cortical cells. PPARα synthetic agonist Wy14643 normalizes the expression of PPARα target genes and restores synaptic activity depressed in hAPP expressing cells. This could result from the proliferation of peroxisomes and/or the expression of peroxisomal enzymes that prevents Aβ-mediated cell death and/or oxidative stress as reported in rat hippocampal and cortical cultures, respectively (72, 73). Moreover, PPARα agonists have been reported to promote the non-amyloidogenic processing of APP in hippocampal neurons by enhancing the expression of the α-secretase ADAM10 that precludes Aβ generation from APP and increases the release of the soluble APP α fragment (74). Therefore, PPARα agonist Wy14643 could promote the nonamyloidogenic processing of APP alleviating therefore the Aβ-mediated negative feedback on synaptic transmission observed in hAPP neurons.

PPARα plays a key role in inflammation and PPAR agonists are anti-inflammatory drugs targeting microglia and astrocytes (11). However, activation of PPARα also produces a strong neuronal signature, by regulating glutamatergic and cholinergic mediated dopaminergic transmission in the brain (75). Although our cortical cells in culture contain both neurons and astrocytes, patch clamp analyses were performed exclusively on neurons, confirming that modulation of the activity of PPARα influences neuronal activity.

Furthermore, we report that PPARα antagonist GW6471 inhibits APP knockdown-induced increases in PPAR activation and synaptic activity in cortical cultures. GW6471 decreases the expression of upregulated *Cpt1a* without modifying the expression of *Acox1* and *Pdk4* of shAPP cells, pointing therefore to differences between Wy14643 and GW6471 in their binding affinity and/or in the recruitment of PPARα nuclear co-activators and/or -repressors (47). However, we report that GW6471 is able to normalize intensive synaptic activity of shAPP

cells. The knock-down of APP in neuronal precursor cells of the hippocampus was previously reported to affect synaptic GluN2B-containing NMDA receptors (76) and PPARα, but not PPARβ and PPARγ was shown to regulate cyclic AMP response element binding and therefore hippocampal plasticity-related genes encoding GluN2A/2B and GluA1 subunits of NMDA and AMPA receptors (16, 17). From these observations, GW6471 could then affect both GluN2B and GluA1 expressions and/or Cpt1c-mediated trafficking of GluA1 (71) to modulate synaptic activity of shAPP neurons. Furthermore, we report that deficiency of PPARα in cortical cells abrogates APP-mediated controls of synaptic activity, confirming that PPARα is an APP-downstream mediator.

A growing body of evidence suggests that synaptic dysfunction may occur long before synapse loss in early AD and may therefore contribute to cognitive dysfunction (3). Abnormalities in brain activity have been reported in both LOAD and EOAD (reviewed in (77)), in which an increased incidence of seizures has been observed, and greater risk for seizures were previously recorded in patients with *APP* duplication and in DS with dementia (78, 79). Spontaneous seizures and sharp wave discharges have been observed in several transgenic models of AD expressing APP mutated or not (32). Moreover, APP overexpression, but not a subsequent Aβ increase, leads to hypersynchronous network activity in an APP transgenic mouse model of AD, suggesting that APP overexpression elicited network alterations through an indirect mechanism (80). Although salutary effects of PPARα and γ agonists on memory have been reported in several preclinical AD models that overexpress APP, human clinical trials using PPARγ agonists in the treatment of AD are less encouraging (reviewed in (10, 37)). A U-shaped relationship between APP level and its functions has been put forward given that both mice overexpressing or lacking APP exhibit, *inter alia*, age-dependent deficits in long-term

potentiation, an activity-dependent enhancement of synaptic strength involved in memory processing (18), learning, vulnerability to seizures and metabolic stress (reviewed in (77)).

As cell energy metabolism and synaptic activity are closely related, it is still questionable whether a PPARα agonist or antagonist could help for synaptic abnormalities associated to cognitive impairments observed in AD. However, our results put forward that the expression of APP as a metabolic regulator should be considered throughout the course of the disease, in which potential APP-mediated metabolic switches driven by PPARα could occur. Moreover, overlapping metabolic dysfunctions reported in AD and metabolic diseases such as obesity and type 2 diabetes (for review see (10)) that have been identified as AD risk factors, emphasize an essential role of lipid and glucose metabolism in the etiology of AD. Therefore, pharmacological modulation of the PPARα metabolic regulator could be part of a personalized multi therapy that could help AD patients, in function of their level of APP expression.

Methods

For cell culture, semiquantitative RT-PCR, immunoblotting analysis, recombinant viruses and cell transduction, an extended section is provided in Supplemental Methods.

Human tissues and animals

Human tissues. Frontal cortex samples from 10 human control subjects and 11 demented patients were analysed. All patients were clinically diagnosed. Neuropathological examinations were performed on multiple formalin fixed, paraffin embedded postmortem frozen brain tissues and confirmed clinically diagnosed patients as late-onset AD cases. Genetic analyses were performed on early-onset AD patients with *APP* microduplication mapping to chromosome 21q2.1, including the APP locus with no contiguous gene. An overview of the donor information and postmortem variables is summarized in Supplemental Tables 1 and 2.

Animals. Pregnant Wistar rats were obtained from the UCLouvain animal facility (Brussels, Belgium) and P0-P1 pups from PPARα deficient (*Ppara*$^{-/-}$) mice (JAX stock #008154) were utilised (81) for embryonic rat and mouse cortical cell cultures, respectively. Age-matched non-transgenic wild type littermates were used as controls. For *Ppara*$^{-/-}$ mice, genotypes were confirmed by PCR amplification from mouse tail biopsies DNA using KAPA Express Extract combined with KAPA2G Robust HotStart Ready Mix (Sopachem, Belgium, #KK7152) by using the following standard Jackson Labs suggested primers (see Supplemental Table 3).

3-4, 6-8 and 11-12 months old transgenic male mice expressing a transgene containing wildtype human APP (APPWT line I5 mouse strain (31) JAX stock #004662) were used. Genotypes were confirmed by PCR amplification with the following standard Jackson Labs suggested primers (see Supplemental Table 3). Mice were group-housed under standardized conditions (12/12 h dark/light cycle, not reversed), with free access to food (SAFE A03, SAFE Diets) and

water *ad libitum*. Temperature in the vivarium was maintained between 20 and 24°C, and humidity between 45 and 65%.

Brain mouse tissue collection. Brains from transgenic mice were snap frozen in liquid nitrogen and stored at −80°C until further use (RNA isolation for RT-qPCR and Western blotting).

Reagents and antibodies. When unmentioned, reagents for cell culture and western blotting were purchased from Thermo Fisher Scientific. Antibodies were purchased as indicated in Supplemental Table 4.

Treatments. At 13-14 DIV, cells were treated for 24 h with 10 µM Wy14643 [[4-Chloro-6-[(2,3-dimethylphenyl)amino]-2-pyrimidinyl]thio]acetic acid (Tocris, #1312), 5µM GW6471 N-((2S)-2-(((1Z)-1-Methyl-3-oxo-3-(4-(trifluoromethyl)phenyl)prop-1-enyl)amino)-3-(4-(2-(5-methyl-2-phenyl-1,3-oxazol-4-yl)ethoxy)phenyl)propyl)propanamide (Tocris, #4618) or vehicle (0.0001% and 0.005% DMSO, respectively). For electrophysiology, cells were treated with 1µM GW6471.

RNA extraction and Real-time PCR. Total RNA was isolated by TriPure Isolation Reagent (Roche, #11667165001) according to the manufacturer's protocol. RNA samples were resuspended in DEPC-treated water (1µg/10µL). Reverse transcription was carried out with the iScript cDNA synthesis Kit (Bio-Rad Laboratories, #1708891) using 1 µg of total RNA in a total volume reaction of 20 µL. Real-time PCR was performed for the amplification of cDNAs with specific primers (Sigma-Aldrich, see Supplemental Table 5). Real-time PCR was carried out in a total volume of 25 µL containing 16 ng cDNA template, 0.3 µM of the appropriate primers and the IQTM SYBR® Green Supermix 1x (Bio-Rad Laboratories, #1708885). The PCR protocol consisted of 40 amplification cycles (95°C for 30 s, 60°C for 45 s and 79°C for

15 s) and was performed using an iCycler IQTM multicolor Real-Time PCR detection system (Bio-Rad Laboratories), used to determine the threshold cycle (Ct). Melting curves were performed to detect nonspecific amplification products. A standard curve was established for each target gene using four-fold serial dilutions (from 100 to 0.097 ng) of a cDNA template mix prepared in the same conditions. Each sample was normalized to relative expression level of ribosomal protein L32 (*Rpl32*). Calculation of Ct, standard curve preparation and quantification of mRNAs in each sample were performed using the "post run data analysis" software provided with the iCycler system (Bio-Rad).

Free fatty acid measurement. Cells in culture (4.10^5 cells / cm^2) were analysed at 13-14 DIV. Total lipids were extracted according to manufacturer guidelines (Free Fatty Acid Quantification Kit, #ab65341, Abcam). Briefly, fatty acids were converted to their CoA derivatives and subsequently oxidized with concomitant generation of color. Octanoate and longer fatty acids were quantified by colorimetric (spectrophotometry at = 570 nm) with detection limit 2 µM free fatty acid in samples. Relative free fatty acids were quantified based on the protein content.

Electrophysiology. Cells in culture (8.10^4 cells / cm^2) were analysed at 13-17 DIV. Total synaptic activity was recorded in voltage-clamp mode (holding potential -60mV). The recording bath solution contained 150 mM NaCl, 5.4 mM KCl, 2 mM CaCl2, 2.1 mM MgCl2, 10 mM HEPES, 10 mM Glucose (pH adjusted to 7.4 with NaOH, osmolarity: 320 mOsm/l at room temperature). Borosilicate glass capillaries were pulled using a P97 horizontal puller (Sutter Instruments) and had a resistance of 4-8 MΩ when filled with the internal solution. The internal pipette solution contained 140 mM KCl, 10 mM EGTA, 10 mM HEPES, 4 mM MgCl2, 0.3 mM GTP and 2 mM ATP-Na_2 (pH adjusted to 7.2 with KOH, 300 mOsm/l). All recordings

were performed at room temperature. Data were acquired using an Axopatch 200B (Axon Instruments), low-pass filtered at 5 kHz and collected at 10 kHz using a Digidata 1322 A digitizer (Axon Instruments). Once whole cell configuration was stablished, liquid junction potential and capacitance transients were compensated. Resting membrane potential measured in current clamp mode (I = 0) was stable and registered using the built-in voltmeter in the Axopatch 200B. Input and series resistance were monitored during the experiment, and recordings were excluded when any of these parameters changed by >10%. Values obtained were annotated in the laboratory protocol notebook. Recordings of total synaptic activity were done for 2 min in a gap-free mode using Clampex 10.1 and analysis was performed offline using Clampfit 10.1 (Axon Instruments) and Excel (Microsoft Corporation).

Statistics. GraphPad Prism (Version 9.0.0 (121) Graph-Pad Software Inc) was used for data display and statistical analysis. We did not predetermine sample sizes. The Shapiro-Wilk test was used to test for the normality of data. Parametric testing procedures (Student's *t*-test or one-way analysis of variance (ANOVA) followed by Tukey's multiple comparison post-test when many subgroups were compared) were applied for normally distributed data, otherwise nonparametric tests were used (Mann-Whitney or Kruskal-Wallis tests followed by Dunn's multiple-comparison post-test when many subgroups were compared). Total number of samples (n) analysed in all experimental conditions (number of repeated measurements) is indicated in figures legends. Results were presented as mean ± SEM and statistical significance was set at P values < 0.05 (two-tailed tests) ($*P<0.05$, $**P<0.01$; $***P<0.001$). In electrophysiology, for non-normally distributed data Kolmogorov-Smirnov test was selected. Values of $P < 0.05$ were considered statistically significant.

Study approval.

Human brain autopsy. Human brain tissues were obtained from the GIE NeuroCEB (Paris) (https://www.neuroceb.org/en/), the Netherlands (Amsterdam) (www.brainbank.nl) and the ULB LHNN (Brussels) Brain Banks. GIE NeuroCEB's Brain Bank procedures have been reviewed and accepted by the Ethical Committee "Comité de Protection des Personnes Paris Ile de France VI" and has been declared to the Ministry of Research and Higher Education as requested by the French law. The Netherlands Brain Bank received permission to perform autopsies and to use tissue and medical records from the Ethical Committee of the VU University Medical Center. Tissues from the ULB LHNN Brain Bank were obtained in compliance and following approval of the Ethical Committee of the Medical School of the Free University of Brussels. An explicit informed consent had been signed by the patient or by the next of kin, in the name of the patient for autopsy and use of their brain tissue for research purposes. **Animals**. All animal procedures used in the study were carried out in accordance with institutional and European guidelines as certified by the local Animal Ethics Committee. Housing conditions were specified by the Belgian Law of 29 May 2013, regarding the protection of laboratory animals (agreement and project numbers: LA2230419 / LA2230652 and 2018/UCL/MD/035).

Author contributions

N.P. supervised the project and edited the final version of the manuscript. N.P. and J-N.O. designed the study. N.P., F.S-O., T.L., F.R. performed the research. A.K., K.L., F.L., E.B, B.S., C.D., P.B; and P.G. contributed the new reagents/analytic tools. N.P., F.S-O. and T.L., analysed the data. N.P. and F.S-O. wrote the manuscript in consultation with J-N.O.

Acknowledgments

We thank the Fondation Louvain for a support to N.P. and the Chilean ANID “Becas Chile” for a support to F.S-O, the Netherlands Brain Bank for providing us with human brain samples. This work was supported by the Belgian Fonds pour la Recherche Scientifique, The Concerted Research Actions, The Belgian Fonds de la Recherche Scientifique Médicale, the Queen Elisabeth Medical Foundation and the Fondation pour la Recherche sur la Maladie d’Alzheimer.

References

1. Lane CA, Hardy J, and Schott JM. Alzheimer's disease. *Eur J Neurol.* 2018;25(1):59-70.
2. DeTure MA, and Dickson DW. The neuropathological diagnosis of Alzheimer's disease. *Molecular Neurodegeneration.* 2019;14(1):32.
3. Selkoe DJ. Alzheimer's disease is a synaptic failure. *Science.* 2002;298(5594):789-91.
4. Bellenguez C, Grenier-Boley B, and Lambert JC. Genetics of Alzheimer's disease: where we are, and where we are going. *Curr Opin Neurobiol.* 2020;61:40-8.
5. Di Paolo G, and Kim TW. Linking lipids to Alzheimer's disease: cholesterol and beyond. *Nat Rev Neurosci.* 2011;12(5):284-96.
6. Picard C, Julien C, Frappier J, Miron J, Theroux L, Dea D, et al. Alterations in cholesterol metabolism-related genes in sporadic Alzheimer's disease. *Neurobiol Aging.* 2018;66:180 e1-e9.
7. Spell C, Kölsch H, Lütjohann D, Kerksiek A, Hentschel F, Damian M, et al. SREBP-1a Polymorphism Influences the Risk of Alzheimer's Disease in Carriers of the ApoE4 Allele. *Dementia and Geriatric Cognitive Disorders.* 2004;18(3-4):245-9.
8. Brune S, Kolsch H, Ptok U, Majores M, Schulz A, Schlosser R, et al. Polymorphism in the peroxisome proliferator-activated receptor alpha gene influences the risk for Alzheimer's disease. *J Neural Transm (Vienna).* 2003;110(9):1041-50.
9. Sjolander A, Minthon L, Bogdanovic N, Wallin A, Zetterberg H, and Blennow K. The PPAR-alpha gene in Alzheimer's disease: lack of replication of earlier association. *Neurobiol Aging.* 2009;30(4):666-8.
10. Saez-Orellana F, Octave JN, and Pierrot N. Alzheimer's Disease, a Lipid Story: Involvement of Peroxisome Proliferator-Activated Receptor alpha. *Cells.* 2020;9(5).
11. Bougarne N, Weyers B, Desmet SJ, Deckers J, Ray DW, Staels B, et al. Molecular Actions of PPARα in Lipid Metabolism and Inflammation. *Endocrine Reviews.* 2018;39(5):760-802.
12. Camandola S, and Mattson MP. Brain metabolism in health, aging, and neurodegeneration. *EMBO J.* 2017;36(11):1474-92.
13. Snowden SG, Ebshiana AA, Hye A, An Y, Pletnikova O, O'Brien R, et al. Association between fatty acid metabolism in the brain and Alzheimer disease neuropathology and cognitive performance: A nontargeted metabolomic study. *PLOS Medicine.* 2017;14(3):e1002266.
14. Hardy J, and Escott-Price V. Genes, pathways and risk prediction in Alzheimer's disease. *Hum Mol Genet.* 2019;28(R2):R235-R40.
15. D'Agostino G, Cristiano C, Lyons DJ, Citraro R, Russo E, Avagliano C, et al. Peroxisome proliferator-activated receptor alpha plays a crucial role in behavioral repetition and cognitive flexibility in mice. *Mol Metab.* 2015;4(7):528-36.
16. Roy A, Jana M, Corbett GT, Ramaswamy S, Kordower JH, Gonzalez FJ, et al. Regulation of cyclic AMP response element binding and hippocampal plasticity-related genes by peroxisome proliferator-activated receptor alpha. *Cell Rep.* 2013;4(4):724-37.
17. Pierrot N, Ris L, Stancu IC, Doshina A, Ribeiro F, Tyteca D, et al. Sex-regulated gene dosage effect of PPARalpha on synaptic plasticity. *Life Sci Alliance.* 2019;2(2).
18. Bliss TV, and Collingridge GL. A synaptic model of memory: long-term potentiation in the hippocampus. *Nature.* 1993;361(6407):31-9.
19. Heneka MT, and Landreth GE. PPARs in the brain. *Biochim Biophys Acta.* 2007;1771(8):1031-45.
20. Chandra S, Roy A, Jana M, and Pahan K. Cinnamic acid activates PPARalpha to stimulate Lysosomal biogenesis and lower Amyloid plaque pathology in an Alzheimer's disease mouse model. *Neurobiol Dis.* 2019;124:379-95.
21. Luo R, Su LY, Li G, Yang J, Liu Q, Yang LX, et al. Activation of PPARA-mediated autophagy reduces Alzheimer disease-like pathology and cognitive decline in a murine model. *Autophagy.* 2020;16(1):52-69.

22. de la Monte SM, and Wands JR. Molecular indices of oxidative stress and mitochondrial dysfunction occur early and often progress with severity of Alzheimer's disease. *J Alzheimers Dis.* 2006;9(2):167-81.
23. Pierrot N, Tyteca D, D'auria L, Dewachter I, Gailly P, Hendrickx A, et al. Amyloid precursor protein controls cholesterol turnover needed for neuronal activity. *EMBO Mol Med.* 2013;5(4):608-25.
24. Zhang S, Hulver MW, McMillan RP, Cline MA, and Gilbert ER. The pivotal role of pyruvate dehydrogenase kinases in metabolic flexibility. *Nutr Metab (Lond).* 2014;11(1):10.
25. Wang W, Zhao F, Ma X, Perry G, and Zhu X. Mitochondria dysfunction in the pathogenesis of Alzheimer's disease: recent advances. *Mol Neurodegener.* 2020;15(1):30.
26. Kao YC, Ho PC, Tu YK, Jou IM, and Tsai KJ. Lipids and Alzheimer's Disease. *Int J Mol Sci.* 2020;21(4).
27. Rovelet-Lecrux A, Hannequin D, Raux G, Le Meur N, Laquerriere A, Vital A, et al. APP locus duplication causes autosomal dominant early-onset Alzheimer disease with cerebral amyloid angiopathy. *Nat Genet.* 2006;38(1):24-6.
28. Selkoe DJ, and Hardy J. The amyloid hypothesis of Alzheimer's disease at 25 years. *EMBO Mol Med.* 2016.
29. Sleegers K, Brouwers N, Gijselinck I, Theuns J, Goossens D, Wauters J, et al. APP duplication is sufficient to cause early onset Alzheimer's dementia with cerebral amyloid angiopathy. *Brain.* 2006;129(Pt 11):2977-83.
30. Esquerda-Canals G, Montoliu-Gaya L, Güell-Bosch J, and Villegas S. Mouse Models of Alzheimer's Disease. *Journal of Alzheimer's Disease.* 2017;57:1171-83.
31. Mucke L, Masliah E, Yu GQ, Mallory M, Rockenstein EM, Tatsuno G, et al. High-level neuronal expression of abeta 1-42 in wild-type human amyloid protein precursor transgenic mice: synaptotoxicity without plaque formation. *J Neurosci.* 2000;20(11):4050-8.
32. Johnson ECB, Ho K, Yu GQ, Das M, Sanchez PE, Djukic B, et al. Behavioral and neural network abnormalities in human APP transgenic mice resemble those of App knock-in mice and are modulated by familial Alzheimer's disease mutations but not by inhibition of BACE1. *Mol Neurodegener.* 2020;15(1):53.
33. Jernberg JN, Bowman CE, Wolfgang MJ, and Scafidi S. Developmental regulation and localization of carnitine palmitoyltransferases (CPTs) in rat brain. *J Neurochem.* 2017;142(3):407-19.
34. Kim YJ, Tu TH, Yang S, Kim JK, and Kim JG. Characterization of Fatty Acid Composition Underlying Hypothalamic Inflammation in Aged Mice. *Molecules.* 2020;25(14).
35. Simon AM, Schiapparelli L, Salazar-Colocho P, Cuadrado-Tejedor M, Escribano L, Lopez de Maturana R, et al. Overexpression of wild-type human APP in mice causes cognitive deficits and pathological features unrelated to Abeta levels. *Neurobiol Dis.* 2009;33(3):369-78.
36. Gonzalez-Dominguez R, Garcia-Barrera T, Vitorica J, and Gomez-Ariza JL. Metabolomic screening of regional brain alterations in the APP/PS1 transgenic model of Alzheimer's disease by direct infusion mass spectrometry. *J Pharm Biomed Anal.* 2015;102:425-35.
37. Wojtowicz S, Strosznajder AK, Jezyna M, and Strosznajder JB. The Novel Role of PPAR Alpha in the Brain: Promising Target in Therapy of Alzheimer's Disease and Other Neurodegenerative Disorders. *Neurochem Res.* 2020;45(5):972-88.
38. Doshina A, Gourgue F, Onizuka M, Opsomer R, Wang P, Ando K, et al. Cortical cells reveal APP as a new player in the regulation of GABAergic neurotransmission. *Sci Rep.* 2017;7(1):370.
39. Schlaepfer IR, and Joshi M. CPT1A-mediated Fat Oxidation, Mechanisms, and Therapeutic Potential. *Endocrinology.* 2020;161(2).
40. Joshi M, Kim J, D'Alessandro A, Monk E, Bruce K, Elajaili H, et al. CPT1A Over-Expression Increases Reactive Oxygen Species in the Mitochondria and Promotes Antioxidant Defenses in Prostate Cancer. *Cancers (Basel).* 2020;12(11).
41. Das SK, Eder S, Schauer S, Diwoky C, Temmel H, Guertl B, et al. Adipose triglyceride lipase contributes to cancer-associated cachexia. *Science.* 2011;333(6039):233-8.

42. Lopez Sanchez MIG, Waugh HS, Tsatsanis A, Wong BX, Crowston JG, Duce JA, et al. Amyloid precursor protein drives down-regulation of mitochondrial oxidative phosphorylation independent of amyloid beta. *Sci Rep.* 2017;7(1):9835.
43. Rakhshandehroo M, Knoch B, Muller M, and Kersten S. Peroxisome proliferator-activated receptor alpha target genes. *PPAR Res.* 2010;2010.
44. Kamenetz F, Tomita T, Hsieh H, Seabrook G, Borchelt D, Iwatsubo T, et al. APP processing and synaptic function. *Neuron.* 2003;37(6):925-37.
45. Ting JT, Kelley BG, Lambert TJ, Cook DG, and Sullivan JM. Amyloid precursor protein overexpression depresses excitatory transmission through both presynaptic and postsynaptic mechanisms. *Proc Natl Acad Sci U S A.* 2007;104(1):353-8.
46. Manczak M, and Reddy PH. RNA silencing of genes involved in Alzheimer's disease enhances mitochondrial function and synaptic activity. *Biochim Biophys Acta.* 2013;1832(12):2368-78.
47. Xu HE, Stanley TB, Montana VG, Lambert MH, Shearer BG, Cobb JE, et al. Structural basis for antagonist-mediated recruitment of nuclear co-repressors by PPARalpha. *Nature.* 2002;415(6873):813-7.
48. Hoyer A, Bardenheuer HJ, Martin E, and Plaschke K. Amyloid precursor protein (APP) and its derivatives change after cellular energy depletion. An in vitro-study. *J Neural Transm (Vienna).* 2005;112(2):239-53.
49. Pottier C, Wallon D, Lecrux AR, Maltete D, Bombois S, Jurici S, et al. Amyloid-beta protein precursor gene expression in alzheimer's disease and other conditions. *J Alzheimers Dis.* 2012;28(3):561-6.
50. Van den Heuvel C, Blumbergs PC, Finnie JW, Manavis J, Jones NR, Reilly PL, et al. Upregulation of amyloid precursor protein messenger RNA in response to traumatic brain injury: an ovine head impact model. *Exp Neurol.* 1999;159(2):441-50.
51. Herbst-Robinson KJ, Liu L, James M, Yao Y, Xie SX, and Brunden KR. Inflammatory Eicosanoids Increase Amyloid Precursor Protein Expression via Activation of Multiple Neuronal Receptors. *Sci Rep.* 2015;5:18286.
52. Haga S, Akai K, and Ishii T. Demonstration of microglial cells in and around senile (neuritic) plaques in the Alzheimer brain. An immunohistochemical study using a novel monoclonal antibody. *Acta Neuropathol.* 1989;77(6):569-75.
53. Jonsson T, Stefansson H, Steinberg S, Jonsdottir I, Jonsson PV, Snaedal J, et al. Variant of TREM2 associated with the risk of Alzheimer's disease. *N Engl J Med.* 2013;368(2):107-16.
54. Sorbi S, Bird ED, and Blass JP. Decreased pyruvate dehydrogenase complex activity in Huntington and Alzheimer brain. *Ann Neurol.* 1983;13(1):72-8.
55. Yellen G. Fueling thought: Management of glycolysis and oxidative phosphorylation in neuronal metabolism. *J Cell Biol.* 2018;217(7):2235-46.
56. Sugden MC, Kraus A, Harris RA, and Holness MJ. Fibre-type specific modification of the activity and regulation of skeletal muscle pyruvate dehydrogenase kinase (PDK) by prolonged starvation and refeeding is associated with targeted regulation of PDK isoenzyme 4 expression. *Biochem J.* 2000;346 Pt 3:651-7.
57. Berger J, Dorninger F, Forss-Petter S, and Kunze M. Peroxisomes in brain development and function. *Biochim Biophys Acta.* 2016;1863(5):934-55.
58. Yao J, Rettberg JR, Klosinski LP, Cadenas E, and Brinton RD. Shift in brain metabolism in late onset Alzheimer's disease: implications for biomarkers and therapeutic interventions. *Mol Aspects Med.* 2011;32(4-6):247-57.
59. Lott IT, and Head E. Dementia in Down syndrome: unique insights for Alzheimer disease research. *Nat Rev Neurol.* 2019;15(3):135-47.
60. Dierssen M, Fructuoso M, Martinez de Lagran M, Perluigi M, and Barone E. Down Syndrome Is a Metabolic Disease: Altered Insulin Signaling Mediates Peripheral and Brain Dysfunctions. *Front Neurosci.* 2020;14:670.
61. Chapel-Crespo CC, Lala S, and Prasun P. Severe Brain Malformations in an Infant With Pyruvate Dehydrogenase Deficiency and Down Syndrome. *Pediatr Neurol.* 2017;75:101-2.

62. Song HJ, Park J, Seo SR, Kim J, Paik SR, and Chung KC. Down syndrome critical region 2 protein inhibits the transcriptional activity of peroxisome proliferator-activated receptor beta in HEK293 cells. *Biochem Biophys Res Commun.* 2008;376(3):478-82.
63. Cimini A, Moreno S, D'Amelio M, Cristiano L, D'Angelo B, Falone S, et al. Early biochemical and morphological modifications in the brain of a transgenic mouse model of Alzheimer's disease: a role for peroxisomes. *J Alzheimers Dis.* 2009;18(4):935-52.
64. Fanelli F, Sepe S, D'Amelio M, Bernardi C, Cristiano L, Cimini A, et al. Age-dependent roles of peroxisomes in the hippocampus of a transgenic mouse model of Alzheimer's disease. *Mol Neurodegener.* 2013;8:8.
65. Bielarczyk H, Jankowska-Kulawy A, Hofling C, Ronowska A, Gul-Hinc S, Rossner S, et al. AbetaPP-Transgenic 2576 Mice Mimic Cell Type-Specific Aspects of Acetyl-CoA-Linked Metabolic Deficits in Alzheimer's Disease. *J Alzheimers Dis.* 2015;48(4):1083-94.
66. Jha MK, Jeon S, and Suk K. Pyruvate Dehydrogenase Kinases in the Nervous System: Their Principal Functions in Neuronal-glial Metabolic Interaction and Neuro-metabolic Disorders. *Curr Neuropharmacol.* 2012;10(4):393-403.
67. Edmond J. Energy metabolism in developing brain cells. *Can J Physiol Pharmacol.* 1992;70 Suppl:S118-29.
68. Hall CN, Klein-Flugge MC, Howarth C, and Attwell D. Oxidative phosphorylation, not glycolysis, powers presynaptic and postsynaptic mechanisms underlying brain information processing. *J Neurosci.* 2012;32(26):8940-51.
69. Priller C, Bauer T, Mitteregger G, Krebs B, Kretzschmar HA, and Herms J. Synapse formation and function is modulated by the amyloid precursor protein. *J Neurosci.* 2006;26(27):7212-21.
70. Czeczor JK, Genders AJ, Aston-Mourney K, Connor T, Hall LG, Hasebe K, et al. APP deficiency results in resistance to obesity but impairs glucose tolerance upon high fat feeding. *J Endocrinol.* 2018;237(3):311-22.
71. Gratacos-Batlle E, Yefimenko N, Cascos-Garcia H, and Soto D. AMPAR interacting protein CPT1C enhances surface expression of GluA1-containing receptors. *Front Cell Neurosci.* 2014;8:469.
72. Santos MJ, Quintanilla RA, Toro A, Grandy R, Dinamarca MC, Godoy JA, et al. Peroxisomal proliferation protects from beta-amyloid neurodegeneration. *J Biol Chem.* 2005;280(49):41057-68.
73. Cimini A, Benedetti E, D'Angelo B, Cristiano L, Falone S, Di Loreto S, et al. Neuronal response of peroxisomal and peroxisome-related proteins to chronic and acute Abeta injury. *Curr Alzheimer Res.* 2009;6(3):238-51.
74. Corbett GT, Gonzalez FJ, and Pahan K. Activation of peroxisome proliferator-activated receptor alpha stimulates ADAM10-mediated proteolysis of APP. *Proc Natl Acad Sci U S A.* 2015;112(27):8445-50.
75. Melis M, Scheggi S, Carta G, Madeddu C, Lecca S, Luchicchi A, et al. PPARalpha regulates cholinergic-driven activity of midbrain dopamine neurons via a novel mechanism involving alpha7 nicotinic acetylcholine receptors. *J Neurosci.* 2013;33(14):6203-11.
76. Pousinha PA, Mouska X, Raymond EF, Gwizdek C, Dhib G, Poupon G, et al. Physiological and pathophysiological control of synaptic GluN2B-NMDA receptors by the C-terminal domain of amyloid precursor protein. *Elife.* 2017;6.
77. Hefter D, Ludewig S, Draguhn A, and Korte M. Amyloid, APP, and Electrical Activity of the Brain. *Neuroscientist.* 2020;26(3):231-51.
78. Cabrejo L, Guyant-Marechal L, Laquerriere A, Vercelletto M, De la Fourniere F, Thomas-Anterion C, et al. Phenotype associated with APP duplication in five families. *Brain.* 2006;129(Pt 11):2966-76.
79. Menendez M. Down syndrome, Alzheimer's disease and seizures. *Brain Dev.* 2005;27(4):246-52.

80. Born HA, Kim JY, Savjani RR, Das P, Dabaghian YA, Guo Q, et al. Genetic suppression of transgenic APP rescues Hypersynchronous network activity in a mouse model of Alzeimer's disease. *J Neurosci.* 2014;34(11):3826-40.
81. Lee SS, Pineau T, Drago J, Lee EJ, Owens JW, Kroetz DL, et al. Targeted disruption of the alpha isoform of the peroxisome proliferator-activated receptor gene in mice results in abolishment of the pleiotropic effects of peroxisome proliferators. *Mol Cell Biol.* 1995;15(6):3012-22.

Figures and figure legends

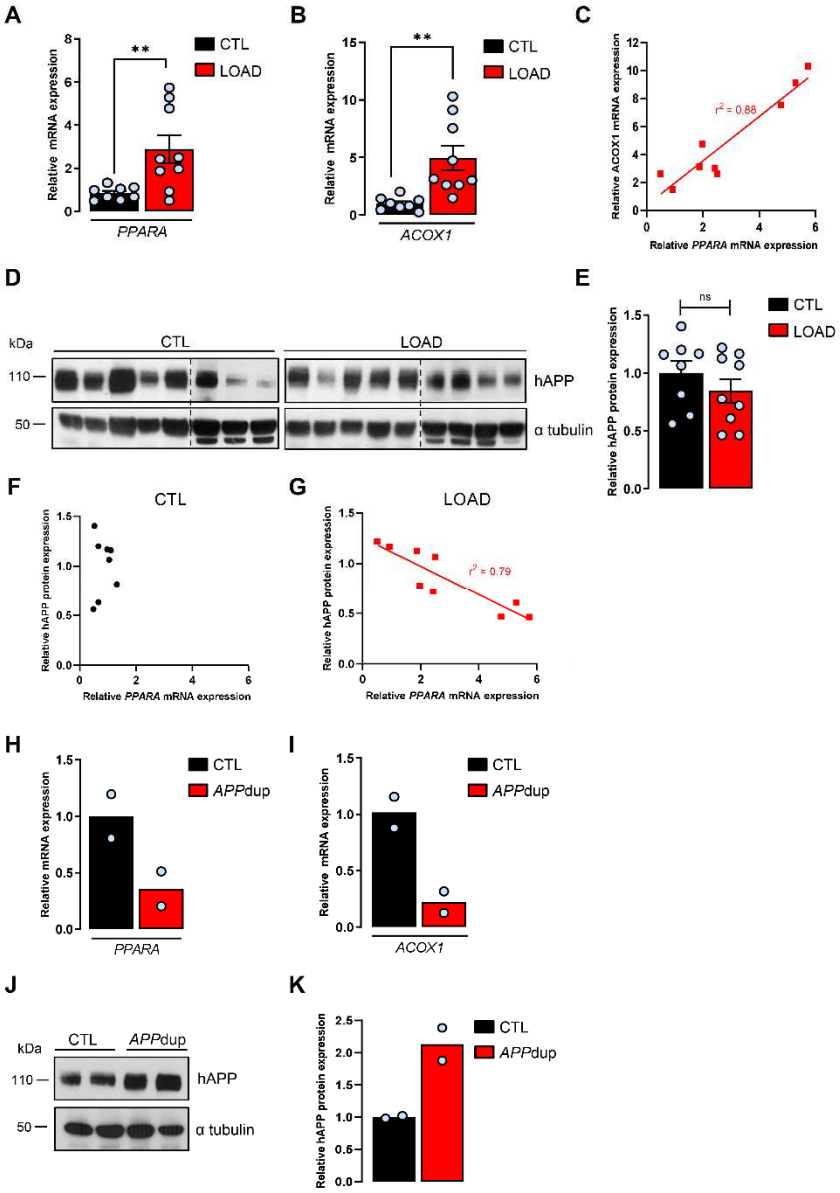

Figure 1. *PPARA* expression and PPARα downstream target genes in brains from patients with Alzheimer disease. Frontal cortex of postmortem human brain tissues from late-onset (LOAD, n = 9) and early-onset Alzheimer disease cases with an *APP* duplication locus (*APP*dup, n = 2) and respective control subjects (CTL in LOAD and *APP*dup cases, n = 8 and 2, respectively) were analysed. (**A**, **B, H** and **I**) Quantitative real time PCR analyses for *PPARA* and *ACOX1* mRNA levels. Results were normalized to *ACTB* mRNA and relative differences are expressed according to respective CTL as mean ± SEM (LOAD: *PPARA* mRNA, $P = 0.009$, *ACOX1* mRNA, $P = 0.003$; Student's t-test). (**C**) mRNA correlation between *ACOX1* and *PPARA* in LOAD. (**D**, **J**) Human APP (hAPP) expression in human brain lysates by immunoblot analysis (see complete unedited blots in the supplemental material). (**E**, **K**) Relative density of hAPP expression compared with α-tubulin. Results were normalized compared to respective CTL and are shown as mean ± SEM. A Student's t-test (LOAD: hAPP protein, $P = 0.0608$) was used to assess significance of the mean. (**F**, **G**) Quantification of hAPP densitometry arbitrary units indicating an inverse correlation between hAPP expression and *PPARA* levels in LOAD. $^{**}P < 0.01$ and non-significant (ns) $P > 0.05$.

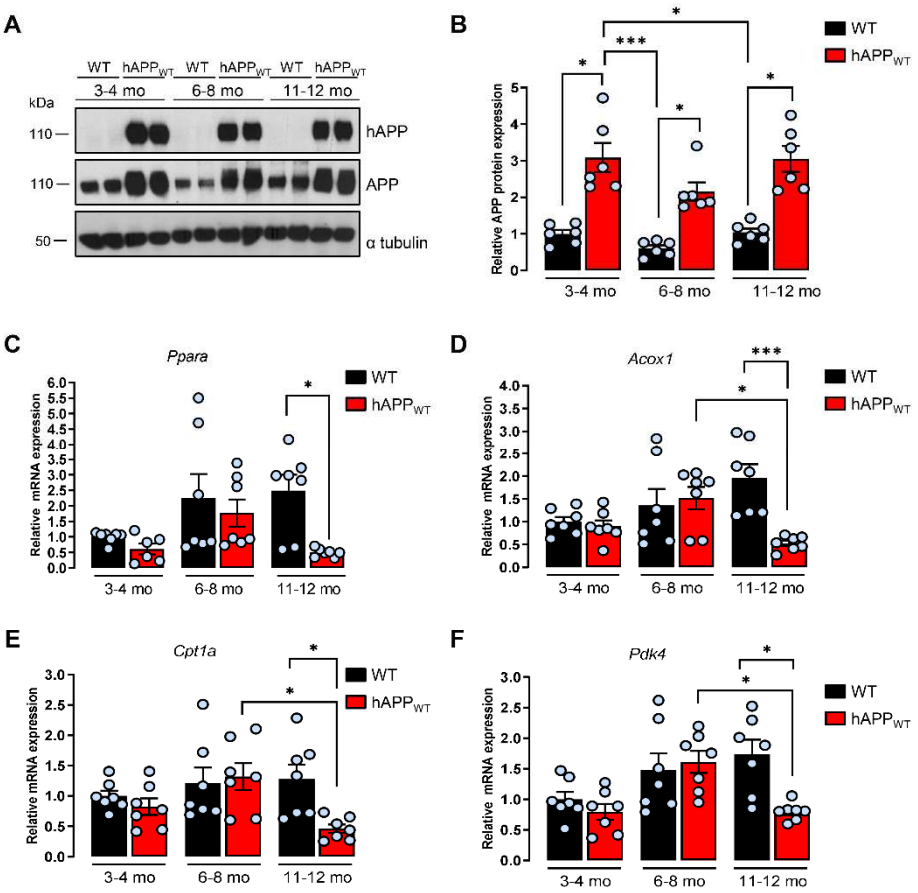

Figure 2. Human APP expression decreases *Ppara* expression and PPARα downstream target genes in old mice. Brain frontal cortex tissues from transgenic mice overexpressing non-mutated human APP ($hAPP_{WT}$) and wild type (WT) littermates were analysed at 3-4, 6-8 and 11-12 months old (mo). (**A**) The expression of hAPP was investigated in mice brain lysates (n = 6 of each) by immunoblot analysis (see complete unedited blots in the supplemental material) with the specific WO2 antibody recognizing hAPP and anti-APP C-terminal antibody recognizing both hAPP and endogenous APP (APP). Blots were further probed using anti-α tubulin antibody. (**B**) Relative density of APP expression was compared with α-tubulin. Results were normalized compared to 3-4 mo WT and are shown as mean ± SEM. A Kruskal-Wallis test followed by Dunn's multiple comparisons post-test was used to assess significance of the mean (APP protein expression at 3-4, 6-8 and 11-12 mo, $P < 0.05$). (**C-F**) Quantitative real time PCR analyses (n = 7 of each) for *Ppara*, *Acox1*, *Cpt1a* and *Pdk4* mRNA levels. Results were normalized to *Rpl32* mRNA, compared to 3-4 mo WT and shown as mean ± SEM. A Kruskal-Wallis test followed by Dunn's multiple comparisons post-test was used to assess significance of the mean (11-12 mo $hAPP_{WT}$ mice: *Ppara* mRNA, $P = 0.012$, *Acox1* mRNA, $P = 0.0008$, *Cpt1a* mRNA, $P = 0.031$; *Pdk4* mRNA, $P = 0.022$), $*P < 0.05$, $***P < 0.001$.

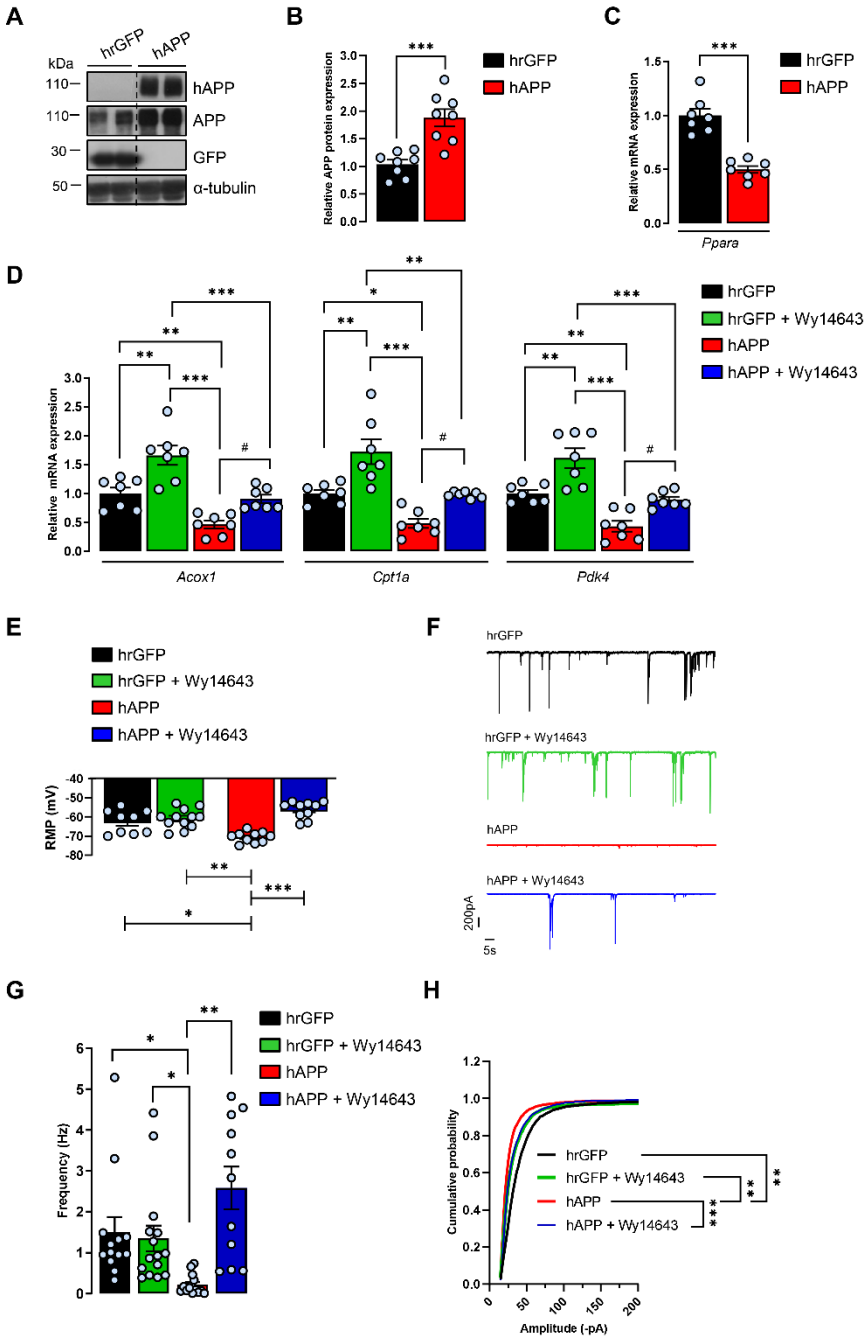

Figure 3. Pharmacological PPARα activation with the Wy14643 prevents human APP-induced decreases in the expression of PPARα target genes and synaptic activity in cortical cultures. Primary cultures of rat cortical cells expressing human recombinant GFP (hrGFP) or APP (hAPP) treated (+) or not (–) with 10µM PPARα agonist Wy14643 for 24h at 13-14 DIV. (**A**) Representative immunoblot of cell lysates (4 independent experiments). The lanes were run on the same gel but were noncontiguous. (**B**) APP expression / α tubulin ratios (n = 8 of each analysed in 4 independent experiments) compared to hrGFP control cells (mean ± SEM); Student's t-test (APP protein, $P = 0.0608$). (**C, D**) Real time PCR analyses for *Ppara*, *Acox1*, *Cpt1a* and *Pdk4* mRNA levels (n = 7 of each analysed in 4 independent experiments). Results were normalized to *Rpl32* mRNA and compared to respective untreated (–) hrGFP control cells. Results are shown as mean ± SEM; one-way ANOVA followed by Tukey's multiple comparisons test ((–) hAPP vs (–) hrGFP: *Ppara* mRNA, $P < 0.0001$, *Acox1* mRNA,

$P = 0.009$, *Cpt1a* mRNA, $P = 0.026$; *Pdk4* mRNA, $P = 0.003$; (+) hAPP vs (–) hAPP: *Acox1* mRNA, $P = 0.039$, *Cpt1a* mRNA, $P = 0.035$; *Pdk4* mRNA, $P = 0.022$). (**E**) Resting membrane potential (RMP) (n = 13-15 cells per group analysed in 5 independent experiments). (**F**) Representative traces of total synaptic activity and (**G**) mean values of synaptic events frequency (n = 15-24 cells per group analysed in 6 independent experiments). (**H**) Cumulative probability plot of the amplitude distribution (n = 15-25 cells per group in 6 independent experiments). (**E - H**) Brown-Forsythe and Welch ANOVA tests followed by Dunnett's T3 multiple comparisons test. $^{*}P < 0.05$, $^{**}P < 0.01$, $^{***}P < 0.001$, $^{\#}P < 0.05$.

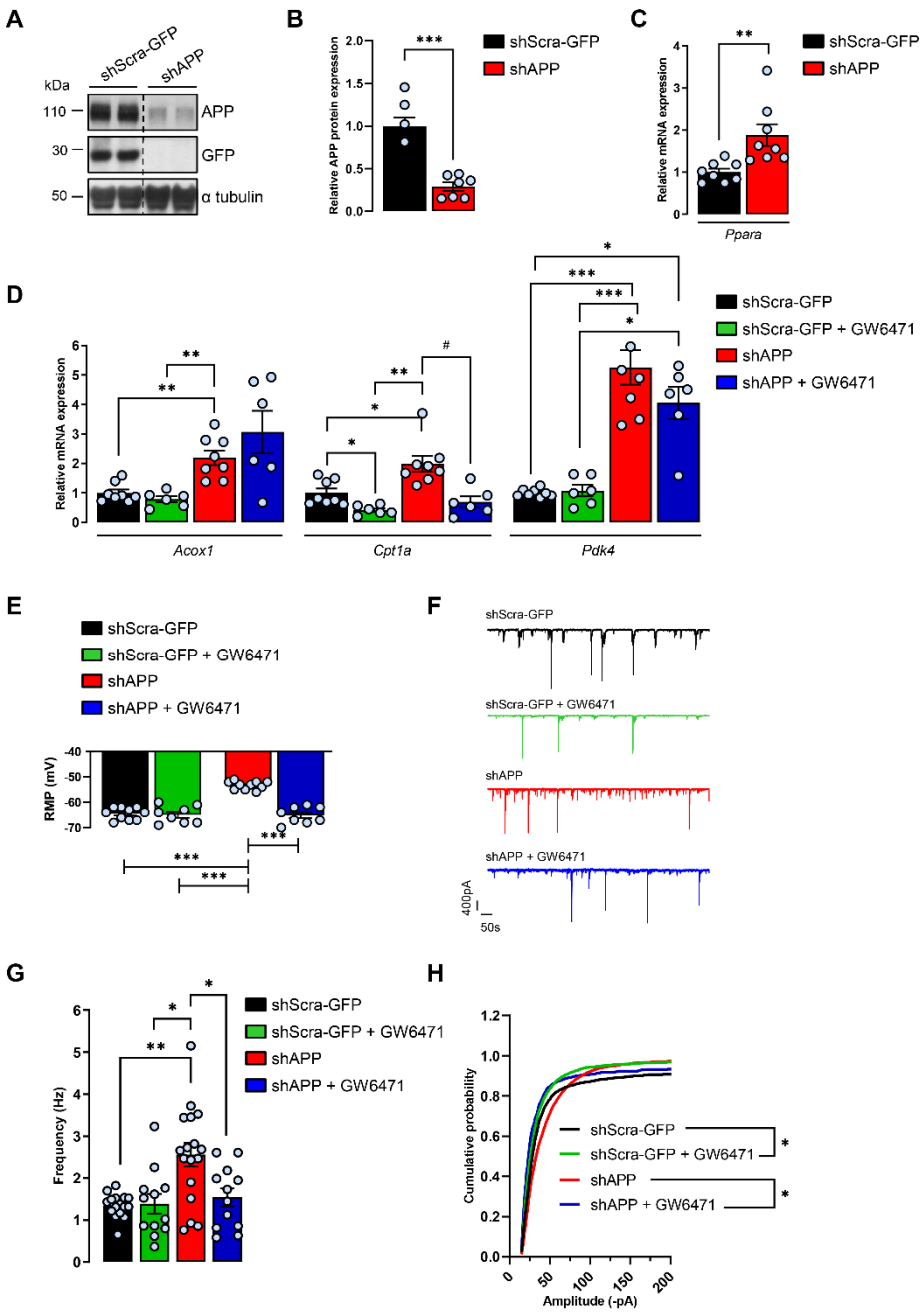

Figure 4. Pharmacological PPARα inhibition with the GW6471 prevents APP knockdown-induced increases in the expression of PPARα target genes and synaptic activity in cortical cultures. Primary cultures of rat cortical cells expressing a shRNA targeting endogenous APP (shAPP) or a scrambled shRNA encoding GFP (shScra-GFP). At 13-14 DIV, cells were treated (+) or not (–) with PPARα antagonist GW6471 for 24h. (**A**) Representative immunoblot of cell lysates, 4 independent experiments (the lanes were run on the same gel but were noncontiguous). (**B**) APP expression / α tubulin ratios (n = 7 of each analysed in 4 independent experiments), mean ± SEM; Student's t-test (APP protein, $P < 0.001$). (**C** and **D**) Real time PCR analyses for *Ppara*, *Acox1*, *Cpt1a* and *Pdk4* mRNA levels (n = 6-8 for each condition analysed in 6 independent experiments). Results were normalized to *Rpl32* mRNA and compared to respective untreated (–) shScra-GFP control cells. Results are shown as mean ± SEM; Brown-Forsythe and Welch ANOVA tests followed by Dunnett's T3 multiple comparisons test ((–) shAPP vs (–) shScra-GFP: *Ppara* mRNA, $P = 0.006$, *Acox1* mRNA, $P =$

0.008, *Cpt1a* mRNA, $P = 0.043$; *Pdk4* mRNA, $P = 0.0009$; (+) shScra-GFP vs (–) shScra-GFP: *Cpt1a* mRNA, $P = 0.026$; (+) shAPP vs (–) shAPP: *Cpt1a* mRNA, $P = 0.010$). (**E**) Resting membrane potential (RMP) (n = 8-10 cells per group analysed in 3 independent experiments). (**F**) Representative traces of total synaptic activity and (**G**) mean values of synaptic events frequency (n = 12-17 cells per group analysed in 6 independent experiments). (**H**) Cumulative probability plot of the amplitude distribution (n = 15-27 cells per group in 7 independent experiments). (**E - H**) Brown-Forsythe and Welch ANOVA tests followed by Dunnett's T3 multiple comparisons test. $^{*}P < 0.05$, $^{**}P < 0.01$, $^{***}P < 0.001$, $^{\#}P < 0.05$.

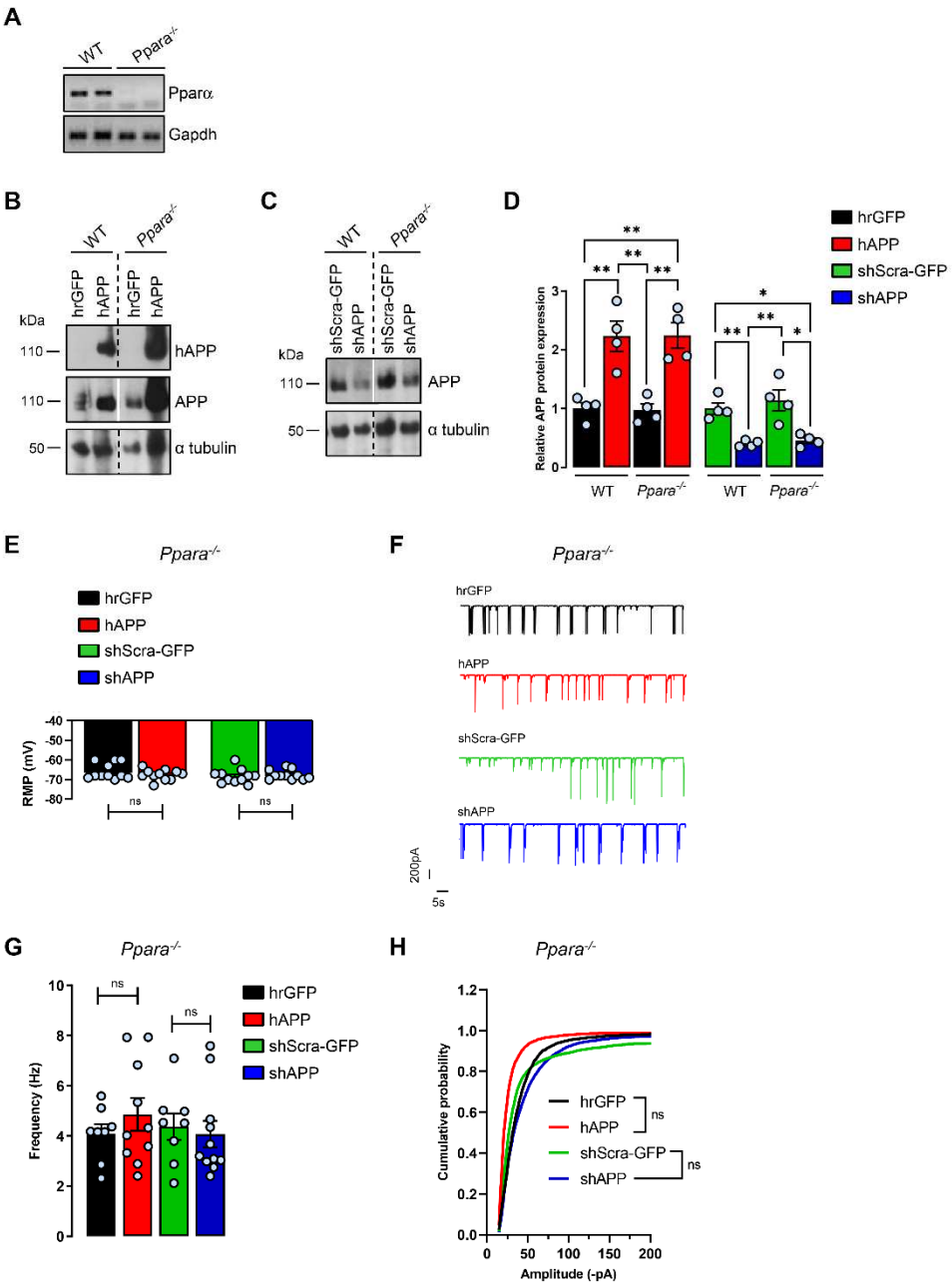

Figure 5. Control of synaptic activity by APP in cortical cultures disappears in absence of PPARα. Primary cultures of mouse cortical cells prepared from wild type (WT) and *Ppara* deficient *(Ppara*$^{-/-}$*)* mice and infected with recombinant adenoviruses encoding human recombinant GFP (hrGFP) or APP (hAPP) proteins or with lentiviruses encoding a shRNA construct designed to target endogenous APP (shAPP) or a scrambled shRNA encoding GFP (shScra-GFP). (**A**) At 13-14 DIV, absence of PPARα expression in cultured cells was assessed by measuring *Ppara* mRNA levels by semi-quantitative RT-PCR. (**B**, **C**) Representative immunoblots of cell lysates, 3 independent experiments (the lanes were run on the same gel but were noncontiguous). The expression of hAPP was monitored with the specific WO2 antibody recognizing hAPP and anti-APP C-terminal antibody recognizing both hAPP and endogenous APP (APP). Immunoblots were further probed using anti-GFP and -α tubulin antibodies. (**D**) APP expression / α tubulin ratios (n = 4 of each) compared to hrGFP or shScra-GFP WT cells (mean ± SEM); One-way ANOVA followed by Tukey's multiple comparisons test (APP

protein: WT and *Ppara*$^{-/-}$ hAPP $P = 0.002$; WT and *Ppara*$^{-/-}$ *s*hAPP, $P = 0.008$ and $P = 0.015$, respectively). (**E**) Resting membrane potential (RMP) measured in WT and *Ppara*$^{-/-}$ transduced neurons (n = 11 cells per group analysed in 3 independent experiments). (**F**) Representative traces of total synaptic activity and (**G**) mean values of synaptic events frequency (n = 8-11 cells per group analysed in 3 independent experiments. (**H**) Cumulative probability plot of the amplitude distribution (n = 10-20 cells per group in 3 independent experiments) measured in WT and *Ppara*$^{-/-}$ transduced neurons. (**E** - **H**) Brown-Forsythe and Welch ANOVA tests followed by Dunnett's T3 multiple comparisons test. *$P < 0.05$, **$P < 0.01$, ***$P < 0.001$ and non-significant (ns) $P > 0.05$.